Differential Effects of Sphingosine 1–Phosphate Receptors on Airway and Vascular Barrier Function in the Murine Lung

Saad Sammani[1], Liliana Moreno-Vinasco[1], Tamara Mirzapoiazova[1], Patrick A. Singleton[1], Eddie T. Chiang[1], Carrie L. Evenoski[1], Ting Wang[1], Biji Mathew[1], Aliya Husain[2], Jaideep Moitra[1], Xiaoguang Sun[1], Luis Nunez[1], Jeffrey R. Jacobson[1], Steven M. Dudek[1], Viswanathan Natarajan[1], and Joe G. N. Garcia[1]

[1]Department of Medicine, and [2]Department of Pathology, Pritzker School of Medicine, University of Chicago, Chicago, Illinois

The therapeutic options for ameliorating the profound vascular permeability, alveolar flooding, and organ dysfunction that accompanies acute inflammatory lung injury (ALI) remain limited. Extending our previous finding that the intravenous administration of the sphingolipid angiogenic factor, sphingosine 1–phosphate (S1P), attenuates inflammatory lung injury and vascular permeability via ligation of $S1PR_1$, we determine that a direct intratracheal or intravenous administration of S1P, or a selective S1P receptor ($S1PR_1$) agonist (SEW-2871), produces highly concentration-dependent barrier-regulatory responses in the murine lung. The intratracheal or intravenous administration of S1P or SEW-2871 at < 0.3 mg/kg was protective against LPS-induced murine lung inflammation and permeability. However, intratracheal delivery of S1P at 0.5 mg/kg (for 2 h) resulted in significant alveolar–capillary barrier disruption (with a 42% increase in bronchoalveolar lavage protein), and produced rapid lethality when delivered at 2 mg/kg. Despite the greater selectivity for $S1PR_1$, intratracheally delivered SEW-2871 at 0.5 mg/kg also resulted in significant alveolar–capillary barrier disruption, but was not lethal at 2 mg/kg. Consistent with the $S1PR_1$ regulation of alveolar/vascular barrier function, wild-type mice pretreated with the $S1PR_1$ inverse agonist, SB-649146, or $S1PR_1^{+/-}$ mice exhibited reduced S1P/SEW-2871–mediated barrier protection after challenge with LPS. In contrast, $S1PR_2^{-/-}$ knockout mice as well as mice with reduced $S1PR_3$ expression (via silencing S1PR3-containing nanocarriers) were protected against LPS-induced barrier disruption compared with control mice. These studies underscore the potential therapeutic effects of highly selective $S1PR_1$ receptor agonists in reducing inflammatory lung injury, and highlight the critical role of the S1P delivery route, $S1PR_1$ agonist concentration, and $S1PR_1$ expression in target tissues.

Keywords: SEW-2871; LPS; SB-649146; S1P; lung edema

Acute lung injury (ALI), a significant cause of morbidity and mortality, is characterized by a diffuse inflammatory parenchymal process, often occurring in the context of multisystem organ failure. Although the exact pathogenetic mechanisms remain poorly defined, multiple risk factors for ALI have been identified, with bacterial sepsis a common predisposing clinical condition (1–3). An essential feature of the inflammatory response in ALI is the disruption of lung endothelial barrier integrity with paracellular gap formation, a consequence of lung endothelial activation by diverse bioactive and biophysical stimuli. Lung vascular barrier dysfunction contributes to high-permeability pulmonary edema and alveolar flooding and extensive leukocyte infiltration into lung tissues, resulting in profound hypoxemia and the requirement for implementing mechanical ventilation (4). Increased vascular permeability in ALI is intimately involved with the development of multisystem organ dysfunction involving distal organs such as the kidney, liver, and intestine, and represents an important independent risk factor for ALI mortality (4–8). Despite intense research and multiple therapeutic trials with diverse targets, specific therapies to prevent or reverse the severe pulmonary inflammation and increased capillary permeability remain elusive.

CLINICAL RELEVANCE

Our study underscores the potential therapeutic effects of highly selective sphingosine 1–phosphate receptor ($S1PR_1$) agonists in reducing inflammatory lung injury, and highlights the critical role of the sphingosine 1–phosphate delivery route, $S1PR_1$ agonist concentration, and $S1PR_1$ expression in the lungs.

A sphingolipid, sphingosine 1–phosphate (S1P), is the metabolic product of sequential sphingomyelinase, ceramidase, and sphingosine kinase enzymatic activities, and represents a vitally important angiogenic factor (38) and signaling mediator with potent vascular barrier–regulating properties (9). S1P functions extracellularly via receptor ligation (9) of the G-protein–coupled S1P receptors (S1PRs), with the $S1PR_1$ receptor expressed in vascular endothelial cells (9) serving as the major barrier-enhancing S1P receptor. $S1PR_1$ ligation promotes the recruitment of actin cytoskeletal regulatory protein to membrane lipid rafts and G_i-coupled signaling to cytoskeletal elements via Rho family of GTPases-Rac (Rac GTPase) (9–12), resulting in decreased endothelial-cell (EC) permeability (9, 11, 12). In addition, $S1PR_1$ receptor expression is essential for platelet-mediated vascular barrier enhancement, because the inhibition of $S1PR_1$ expression attenuates this effect (13).

Our previous *in vivo* work strongly indicated that S1P produces potent *in vivo* lung vascular barrier enhancement through the ligation of $S1P_1$ receptors in murine and canine models of endotoxin-induced ALI (14, 15), suggesting a novel therapeutic potential for S1P and related compounds in ALI. For example, FTY-720, a structural analogue of S1P and a potent agonist for S1P receptors after phosphorylation by sphingosine kinase, is being evaluated in Phase III clinical trials as an immunosuppressant (16). We and others showed that S1P and FTY-720 potently reverse the vascular permeability induced by vascular endothelial cell growth factor (17), LPS (15), and ischemia–reperfusion injury (18). In contrast to the protective effects of $S1P_1$ ligation, the activation of $S1P_2$ or $S1P_3$ receptors induces significant alveolar and vascular barrier disruption via the $G_{12/13}$-coupled and G_q-coupled activation of Rho/Rho kinase–mediated stress-fiber formation (10–12, 19, 20). In addition, recent reports indicate

(*Received in original form June 23, 2009 and in final form September 3, 2009*)

This study was supported by grants HL 58064 (J.G.N.G.) and HL 79396 (V.N.) from the National Institutes of Health.

Correspondence and requests for reprints should be addressed to Joe G. N. Garcia, M.D., Institute for Personalized Respiratory Medicine, University of Illinois at Chicago, 1705 Polk #305, Chicago, IL 60637. E-mail: jggarcia@uic.edu

Am J Respir Cell Mol Biol Vol 43. pp 394–402, 2010
Originally Published in Press as DOI: 10.1165/rcmb.2009-0223OC on September 11, 2009
Internet address: www.atsjournals.org

adverse S1P-mediated effects on airway responses when markedly elevated concentrations of S1P are delivered intratracheally, possibly a consequence of $S1PR_2$ or $S1PR_3$ ligation, findings that potentially limit the therapeutic utility of S1P (21).

Here, we explored the differential effects of S1P receptors in a murine model of inflammatory lung injury induced by LPS. We determined that the intravenous or intratracheal administration of either S1P or a selective $S1PR_1$ agonist (SEW-2871) up to 0.3 mg/kg ($\sim$ 200 μM) produced dose-dependent alveolar and vascular barrier protection in C57Bl/6 mice. In contrast, the intratracheal delivery of 0.5 mg/kg S1P ($\sim$ 1 mM final plasma concentration) resulted in significant alveolar–capillary barrier disruption, with approximately 50% increase in permeability and inflammatory indices compared with untreated animals. The delivery of markedly elevated concentrations of S1P ($\sim$ 2 mg/kg; $\sim$ 4 mM concentration) was rapidly lethal. Despite greater $S1PR_1$ selectivity, exposures to SEW-2871 at both 0.5 and 2 mg/kg were not lethal but did result in significant alveolar–capillary barrier disruption. $S1PR_1^{+/-}$ heterozygous mice were significantly refractory to the protective effects of S1P ($<$ 0.5 mg/kg), but both $S1PR_2^{-/-}$ knockout (KO) mice and silenced $S1PR_3$ mice were less susceptible to lung injury after challenge with LPS. These studies, designed to assess the potential therapeutic effects of exogenous S1P in inflammatory lung injury, underscore the critical role of the S1P delivery route, concentration, and relative receptor expression, and indicate S1P receptor selectivity as a major driver of S1P and S1P analogue toxicity.

MATERIALS AND METHODS

Mice and Reagents

All experiments and animal-care procedures were approved by the University of Chicago Animal Care and Use Committee. Male C57BL/6 (20–25 g) mice, 8 to 10 weeks old, were purchased from Jackson Laboratory (Bar Harbor, ME) and housed until the time of experiments in cages with free access to food and water in a temperature-controlled room with a 12-hour dark/light cycle. In total, four to five mice were used in each group. S1P was purchased from Avanti Polar Lipids (Alabaster, AL), SEW-2871 was procured from Cayman Chemical Co. (Ann Arbor, MI), LPS was purchased from Sigma (St. Louis, MO), and SB-649146 was obtained from Glaxo Smith Kline (King of Prussia, PA). $S1PR_1^{+/-}$ heterozygous and $S1PR_2^{-/-}$ KO mice were obtained from Dr. Richard L. Proia (National Institutes of Health, Bethesda, MD).

Experimental Model

Mice were anesthetized with an intraperitoneal mix of ketamine (150 mg/kg) and acepromazine (15 mg/kg), as described previously (15), before exposure of the trachea and the right internal jugular vein. For the group of animals exposed to LPS-mediated acute lung injury, *Escherichia coli* 127-B8 endotoxin LPS solution (2.5 mg/kg) or sterile saline was instilled intratracheally via a 20-gauge intravenous catheter. Using the same method, S1P, SEW-2871, or vehicle was injected in the airways 2 hours after the administration of LPS. However, mice received S1P or SEW-2871 or vehicle intravenously via the internal jugular vein simultaneously with the injection of LPS. In the murine group with the $S1P_1$ inverse agonist challenge, SB-649146 or PBS was injected intravenously 30 minutes before the LPS/S1P intravenous injection or LPS/SEW-2871 intravenous injection. Bronchoalveolar lavage (BAL) fluid was collected and lungs were harvested at 18 hours (final time point) and stored at -80°C for evaluations of lung injury.

BAL Protein Accumulation and Leukocyte Quantification

BAL was performed by flushing the lungs with 1 ml of cold Hanks' balanced salt solution (HBSS; Invitrogen, Grand Island, NY) through the tracheal cannula, as previously described (22). The recovered lavage fluid ($\sim$ 0.8 ml) was centrifuged (500 $\times$ *g* for 20 min), and the cell pellet was resuspended in 200 μl of ice-cold HBSS. Total numbers of cells were counted with a hemacytometer. The BAL differential cell count was prepared using cytocentrifugation (Cytospin 3; Shandon Instruments, Pittsburgh, PA), and stained with Diff-Quik (Dade Behring, Düdingen, Switzerland). BAL cell differential counts were determined using morphologic criteria under a light microscope, with an evaluation of approximately 400 cells per slide. The supernatant from BAL fluid was centrifuged again (15,000 $\times$ *g* for 10 min), and the supernatant was stored at -80°C for further protein analysis (15).

Measurements of Total Proteins and Albumin from BAL

Protein concentrations in BAL fluid were measured using an RC DC Protein Assay (Bio-Rad, Hercules, CA) according to the manufacturer's recommendations, as previously described (23). Optical density readings of samples were converted to milligrams/milliliters, using values obtained from a standard curve generated with serial dilutions of BSA (0.1–1.5 mg/ml) (24).

Measurement of Albumin Concentrations and Myeloperoxidase Activity in Lung Tissue

Lung-tissue homogenates were prepared in phosphate buffer (pH 6.0) containing 0.1% hexadecyltrimethyl ammonium bromide (HTAB; Sigma) by homogenization on a Polytron (Qiagen) fitted with a 7-mm probe, as previously described (25). The homogenates were frozen, thawed, and sonicated, and the supernatant was recovered as described elsewhere (25). Extravasation of albumin in the lung parenchyma was determined from the clear supernatant, using sandwich ELISA kits at dilutions of 1:20,000. Neutrophils trapped in the lung parenchyma were monitored from the same tissue extract at 1:100 dilution, using a sandwich ELISA kit specific for mouse myeloperoxidase (MPO) (HyCult Biotechnology, Uden, The Netherlands). Values in terms of concentration (ng/ml) were converted to mass antigen/wet weight of lungs by taking into account the weight of the tissue that was homogenized initially in 1 ml of phosphate–HTAB buffer, as previously described (25).

Lung Histopathology

LPS-mediated alterations in lung morphology were characterized as previously described (24) in excised left lungs (three animals/group) placed immediately in formalin overnight, followed by embedding in paraffin for histological evaluation by hematoxylin–eosin staining. An inflammatory injury score was calculated according to the number of total whiter blood cells (WBCs), and especially polymorphonuclear leukocytes (PMNs), in all study groups. A pathologist (A.N.H.), blinded to study-group delineation, served as the grader of lung-injury severity, assessing each slide for edema, inflammation, and the presence of hyaline membranes, according to the criteria: (*1*) edema: absent, mild (10% alveoli involved), moderate (involving10–50% alveoli), or severe (involving 50% alveoli); (*2*) inflammation: absent, mild (10 inflammatory cells/high-power field [hpf]), moderate (10–50 inflammatory cells/hpf), or severe (50 inflammatory cells/hpf); and (*3*) hyaline membranes: present or absent (26).

Angiotensin 1–Converting Enzyme Antibody–Conjugated Nanocarriers to Deliver $S1P_3$ Short, Interfering RNA

Nanocarriers with polymer shells composed of poly ethylene glycol)-b-poly lactic-glycolic acid (PLA-b-PEG-COOH/PLC-COOH) were prepared and tagged to the angiotensin-converting enzyme (ACE) antibody to ensure the targeting of lung vasculature. The ACE-tagged polymer was combined with the short, interfering (si) STABLE $S1P_3$ siRNA targeting mRNA sequence 5′-GCU UCA UCG UCU UGG AGA A UU-3′ (5.5 μg ACE/mg polymer). The nanocarrier/siRNA mixture was sonicated in a water-bath sonicator (Fisher Scientific, Itasca, IL) to the point of clarity. For the ACE antibody, primary amines were blocked with N-hydroxysulfosuccinimide (sulfo-NHS) acetate in PBS, pH 7.4, and incubated for 1 hour at room temperature. The solution was then filtered with a 30-kD Ultrafree-MC filter (Millipore, Danvers, MA) and adjusted to a final concentration of 0.2 mg/ml. The modified ACE antibody was crosslinked to carriers containing $S1P_3$ siRNA by covalently linking the carboxyl groups in the ACE antibody with the amine groups on polymer, using the EDC reagent (Pierce, Rockford, IL). The solvent was evaporated in a water bath at 50°C under nitrogen. The resulting polymer film was immediately suspended in PBS (pH 7.4; final concentration, 62.5 nM si$S1PR_3$ and 14.7 μg of polymer PLA-b-PEG-COOH/PLC-COOH). A total of 100 μl of

sterile, ACE-conjugated nanocarrier (containing 10 mg/kg siRNA for $S1PR_3$) was injected once into the internal jugular vein of C57B6/6J mice 5 days before harvesting.

RESULTS

Concentration-Dependent and Delivery Route–Dependent Effects of S1P and SEW-2871 on Murine Lung Fluid Balance

To assess the therapeutic potential of $S1PR_1$ ligation as a therapeutic strategy for lung-barrier dysfunction in ALI, our initial experiments evaluated the effects of increasing concentrations of S1P (0.001–2 mg/kg) and the $S1PR_1$ agonist SEW-2871 (0.1–2 mg/kg), as well as the influence of intratracheal and intravenous routes of S1P/SEW-2871 delivery on lung fluid balance in C57Bl/6 male mice. The intratracheal delivery of increasing concentrations of either S1P (0.001–0.1 mg/kg) or SEW-2871 (0.1–0.3 mg/kg) failed to increase BAL total protein concentrations significantly at 2 hours (compared with PBS-challenged control mice) (Table 1). In contrast, compared with untreated animals, the intratracheal delivery of 0.5 mg/kg S1P (estimated $\sim$ 1 mM peak final plasma concentration) resulted in significant alveolar–capillary barrier disruption, with greater than 40% increase in BAL inflammatory indices such as BAL protein (Table 1) ($P \leqslant 0.05$). The intratracheal delivery of S1P at approximately 2 mg/kg (estimated final concentration, $\sim$ 4 mM) was rapidly lethal. In contrast, the intratracheal delivery of SEW-2871 was not lethal at either 0.5 mg/kg or 2 mg/kg. Despite greater $S1PR_1$ selectivity, at these concentrations, SEW-2871 (like S1P) also resulted in significant alveolar–capillary barrier disruption (Table 1).

Consistent with our previous *in vivo* reports on intact mice (14, 15, 18) and isolated perfused murine lungs (14), an intravenous injection of S1P (0.03 mg/kg) via the internal jugular vein to the target pulmonary endothelium significantly reduced the basal BAL total protein accumulation (Table 1), assessed 2 hours after injection. SEW-2871 produced similar dose-dependent basal barrier protection, even when intravenously administered at up to 0.5 mg/kg (Table 1).

Dose-Dependent and Delivery Route–Dependent Effects of S1P and SEW-2871 on LPS-Induced Murine Acute Lung Injury

We next examined the dose-dependent and route-dependent effects of S1P and SEW-2871 delivery in a murine model of LPS-induced ALI. Mice challenged with intratracheal LPS (2.5 mg/kg) demonstrated substantial increases in lung permeability (Table 1 and Figures 1A and 1B). In contrast, mice with intratracheal injection of either S1P (0.001–0.1 mg/kg) or SEW-2871 (0.1–0.3 mg/kg), delivered 2 hours after LPS, exhibited significant reductions in LPS-induced lung inflammation and alveolar edema at 18 hours (Table 1 and Figures 1A and 1B). In addition, consistent with our previous reports (15), targeting $S1PR_1$ receptors in the vasculature by the intravenous administration of S1P (0.03 mg/kg) significantly attenuated vascular leakage and lung inflammation, as reflected by significant decreases in BAL protein and histologic scores, compared with LPS-challenged control mice (Table 1 and Figure 1A). The attenuation of vascular leakage by both intravenously delivered S1P (0.03 mg/kg) and SEW-2871 (0.1–0.3 mg/kg) in the murine model of LPS-induced ALI was dose-dependent ($P < 0.05$) (Table 1 and Figure 1A). Significantly improved histologic injury scores reflected a dramatic reduction of neutrophilic lung infiltration with SEW (Figure 2). In addition to the intravenous and intratracheal delivery routes, SEW (1 mg/kg), administered intraperitoneally in the LPS-induced murine ALI model, produced a significant decrease in BAL inflammatory cells and BAL total protein compared with LPS-treated mice receiving PBS ($n = 4$, data not shown).

Effects of $S1PR_1$ Inverse Agonism or Gene Deletion on S1P/SEW-2871–Mediated Vascular Barrier Protection during LPS-Induced Acute Lung Injury

We next used SB-649146 (0.1 mg/mouse), a novel inverse agonist of $S1PR_1$ that stabilizes the inactive confirmation of this receptor (27), to confirm the role of $S1PR_1$ in S1P-mediated and SEW-2871–mediated barrier enhancement. C57Bl/6 mice received 0.1 mg/mouse of SB-649146 intravenously, 30 minutes before the challenge with LPS. Mice were then challenged with intravenous S1P (0.03 mg/kg) or SEW-2871 (0.1 mg/kg). The administration of 0.1 mg/mouse of SB-649146 attenuated both S1P-mediated and SEW-2871–mediated barrier enhancement with increased BAL total protein concentrations (at 18 hours) (Figures 3A and 3B). By itself, SB-649146 had no effect on BAL protein levels (Figure 3A), suggesting that our low concentration of the inverse agonist did not alter basal endothelial barrier function, but was sufficient to attenuate S1P-induced $S1PR_1$ coupling and signaling.

TABLE 1. DOSE AND ROUTE EFFECTS OF S1P OR SEW-2871 ON LUNG ALVEOLAR PERMEABILITY

Agonist	Intratracheal (2 Hours)	Intratracheal + LPS (18 Hours)	Intravenous (2 Hours)	Intravenous + LPS (18 Hours)
S1P				
Vehicle	0.20 ± 0.01	0.84 ± 0.09‡	0.18 ± 0.02	1.05 ± 0.14‡
0.001 mg/kg	0.22 ± 0.01	0.52 ± 0.16†‡	0.15 ± 0.01	ND
0.03 mg/kg	ND	ND	0.17 ± 0.04	0.64 ± 0.08†‡
0.1 mg/kg	0.23 ± 0.02	0.65 ± 0.02†‡	ND	ND
0.5 mg/kg	0.34 ± 0.03*	ND	0.15 ± 0.01	ND
2 mg/ml	Lethal	ND	ND	ND
SEW-2871				
Vehicle	0.22 ± 0.03	1.01 ± 0.06‡	0.22 ± 0.04	0.95 ± 0.09‡
0.1 mg/kg	0.23 ± 0.05	0.63 ± 0.13†‡	0.18 ± 0.02	0.59 ± 0.1†‡
0.3 mg/kg	0.29 ± 0.06	0.53 ± 0.20†‡	0.15 ± 0.01	0.65 ± 0.15†‡
0.5 mg/kg	0.33 ± 0.03*	ND	0.14 ± 0.01	ND
2 mg/ml	0.36 ± 0.01*	ND	ND	ND

Definitions of abbreviations: S1P, sphingosine 1–phosphate; SEW-2871, selective S1P receptor 1 agonist; ND, not determined.

Values represent protein concentrations in bronchoalveolar lavage (BAL) fluids. Male C57BL/6J mice were challenged with saline (Vehicle), S1P, or SEW-2871, delivered intratracheally or intravenously. BAL fluid was harvested after 2 hours of injection.

* Significant difference between vehicle and 2-hour agonist treatments.

† Significant differences between LPS and LPS/agonist.

‡ Significant differences between 2-hour intratracheal or intravenous drug control and LPS challenge. S1P delivered intratracheally at 2 mg/kg was rapidly lethal.

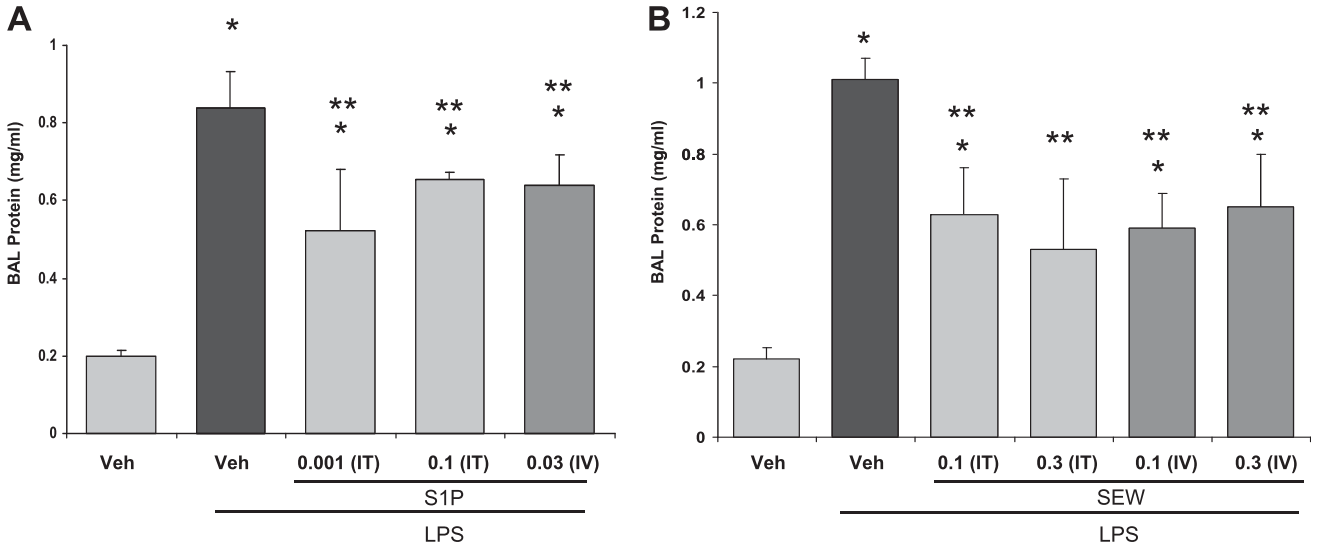

Figure 1. Effects of sphingosine 1–phosphate (S1P) and selective S1P receptor ($S1PR_1$) agonist (SEW-2871) on LPS-induced increases in lung permeability. (*A*) Effects of S1P (0.001 and 0.1 mg/kg) in C57BL/6 mice delivered intratracheally, 2 hours after LPS injection (2.5 mg/kg) and harvested 16 hours later. Bronchoalveolar lavage (BAL) protein accumulation was significantly decreased in S1P-treated mice compared with the LPS-only group (*$P \leq 0.05$). Similarly, intravenously delivered S1P (0.03 mg/kg) produces significant barrier enhancement 18 hours after LPS injection, reflected by decreased BAL protein concentrations (*$P \leq 0.05$ versus vehicle, **$P \leq 0.05$ versus LPS) compared with LPS-treated animals ($n = 5$). Veh, vehicle. (*B*) Results after injection of SEW-2871 (SEW) both intratracheal and intravenous, 0.1 and 0.3 mg/kg, respectively, after LPS injection (2.5 mg/kg) and harvested after 16 and 18 hours, respectively. The accumulation of BAL protein was significantly decreased, reflecting lung barrier function enhancement (*$P \leq 0.05$ versus vehicle, **$P \leq 0.05$ versus LPS).

Effects of LPS on Lung Barrier Function in $S1PR_1^{+/-}$ Mice

To study the specific barrier-enhancing role of $S1PR_1$, wild-type or $S1PR_1^{+/-}$ mice were challenged with LPS, with BAL fluid retrieval and lung harvesting 18 hours after LPS. Clear disruption of vascular barrier integrity was reflected by a significant increase in the BAL PMN cell count in $S1PR1^{+/-}$ mice compared with wild-type mice ($P = 0.03$) (Figure 4A). We also assessed intravenous S1P-mediated barrier enhancement in $S1PR_1^{+/-}$ and wild-type mice exposed to LPS-induced lung injury. S1P failed to preserve or enhance lung barrier function in LPS-stimulated $S1PR_1^{+/-}$ mice, as reflected by increased lung tissue MPO activity, an index of the inflammatory process ($P = 0.01$) (Figure 4B).

Effect of LPS on Lung Barrier Function in Mice with Altered $S1PR_2$ or $S1PR_3$ Expression

To address S1P receptor–specific responses in ALI, wild-type mice and genetically engineered $S1PR_2^{-/-}$ KO mice were exposed to LPS-induced barrier disruption. BAL collected at 18 hours revealed that total protein levels in $S1PR_2^{-/-}$ KO mice were significantly reduced (*$P = 0.02$) compared with wild-type mice, consistent with a barrier-disruptive role of $S1P_2$ receptors (Figure 5A). However, no significant difference was evident in BAL WBC counts (Figure 5B). ACE antibody–conjugated nanocarriers were used to deliver $S1PR_3$ siRNA by daily intravenous injections (5 days before the administration of LPS). BAL analysis 18 hours after the administration of LPS illustrated a barrier-protective effect after $S1PR_3$ silencing, as reflected by Western blot analysis (Figure 6A), with decreases in BAL protein concentrations (Figure 6B) and lung tissue albumin content (Figure 6C) in $S1PR_3$-silenced mice compared with nonsilenced mice ($P < 0.05$ and $P < 0.01$ for LPS versus si$S1PR_3$ vehicle group comparisons).

DISCUSSION

Sphingolipids such as S1P, produced via the phosphorylation of sphingosine by sphingosine kinase, have emerged as important signaling molecules with important vascular regulatory properties. We previously described the capacity for S1P to activate lung endothelium directly (28), and identified S1P as a potent angiogenic factor and major endothelial chemotactic factor in serum (29). A critical observation, however, was establishment of a clear link between angiogenesis and inflammation, with S1P identified as the first angiogenic factor to exert rapid, sustained, and dose-dependent vascular barrier enhancement (9), an attribute afterward ascribed to other angiogenic factors such as hepatocyte growth factor and angiopoietin-1 (30). We subsequently described a signaling cascade evoked by S1P receptor ligation that leads to a reorganization of the vascular EC cytoskeleton and enhanced junctional integrity (11, 12, 31), that is, biophysical events that ultimately strengthen the EC barrier and decrease vascular permeability (19, 32–35).

Because effective therapies to reduce the profound vascular leakage in ALI are severely limited, considerable interest has arisen regarding *in vivo* investigations with intravenously delivered S1P as a potentially effective therapy for reducing vascular leakage in inflammatory lung injury (15). In these studies, intravenous S1P significantly attenuated LPS-induced lung injury in spontaneously respiring mice (15), and markedly improved oxygenation and alveolar edema resolution in mechanically ventilated dogs in a combined injury model of intrabronchial LPS instillation and ventilator-induced lung injury (14). However, relevant to the potential use of S1P as an ALI therapeutic strategy is the continuous exposure of the microcirculation to activating levels of S1P (S1P is found in nanomolar quantities in plasma) (36). This finding suggests that the dynamic expression of G-protein–coupled S1PRs is likely a major mechanism that coordinates S1P-mediated cellular responses, including vascular barrier regulation. Not all S1P receptors are barrier-enhancing, and conflicting or controversial roles of specific S1PRs in vascular homeostasis were postulated (12, 21, 37), findings that contributed to a potential limitation for S1P and related analogues as therapeutic strategies in acute inflammatory lung disorders. For example, although the intravascular administra-

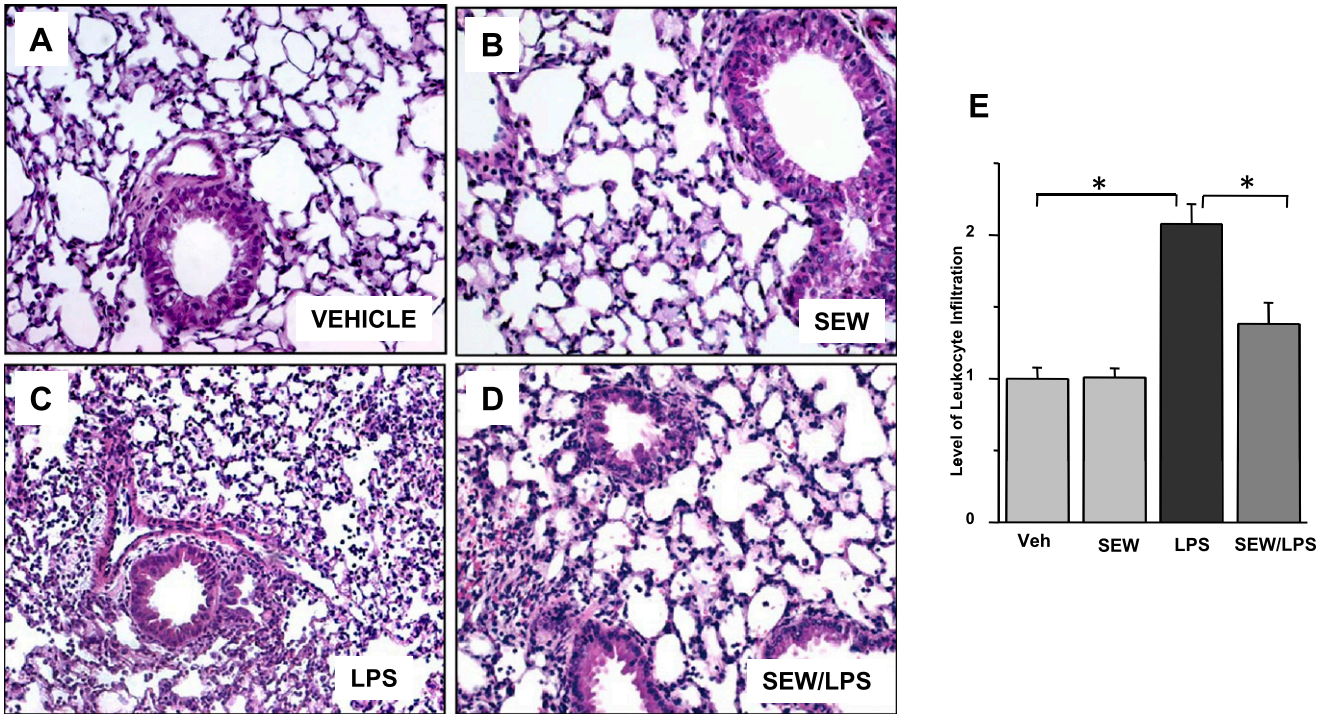

Figure 2. Histologic evaluation of barrier enhancement properties of SEW-2871 in LPS-induced acute lung injury. Sections were stained with hematoxylin–eosin for histologic evaluations of vehicle (*A*) and SEW-2871 (*B*), respectively, without evidence of inflammation. (*C*) In contrast, histologic assessments of LPS-mediated barrier dysfunction revealed a moderate increase in infiltrating polymorphonuclear leukocytes (PMNs) in lung tissue and prominent increases in alveolar edema. (*D*) These LPS-mediated histologic alterations were attenuated by treatment with SEW-2871. (*E*) Relative levels of leukocyte infiltration, quantified as aggregated histologic scores, reflect SEW-2871–mediated decreases in leukocyte influx compared with LPS alone.

tion of S1P (< 1 μM or 85 μg/kg) protects against the inflammatory injury associated with ALI, elevated concentrations of S1P (> 5–10 μM) produce substantial endothelial cell barrier disruption *in vitro*, possibly via the ligation of S1PRs other than $S1PR_1$ (11). Moreover, adverse S1P-mediated effects on airway responses were evident when S1P was delivered intratracheally (21, 38). Those report depicted lung edema 2 hours after the intratracheal injection of 2 mg/kg of S1P. Our data and earlier reports clearly demonstrate that despite the abundant expression of $S1PR_1$, $S1PR_2$, and $S1PR_3$ in lung tissue and lung vascular endothelium, only the ligation of $S1PR_1$ reduces murine lung vascular permeability in response to LPS (15), ischemia/reperfu-

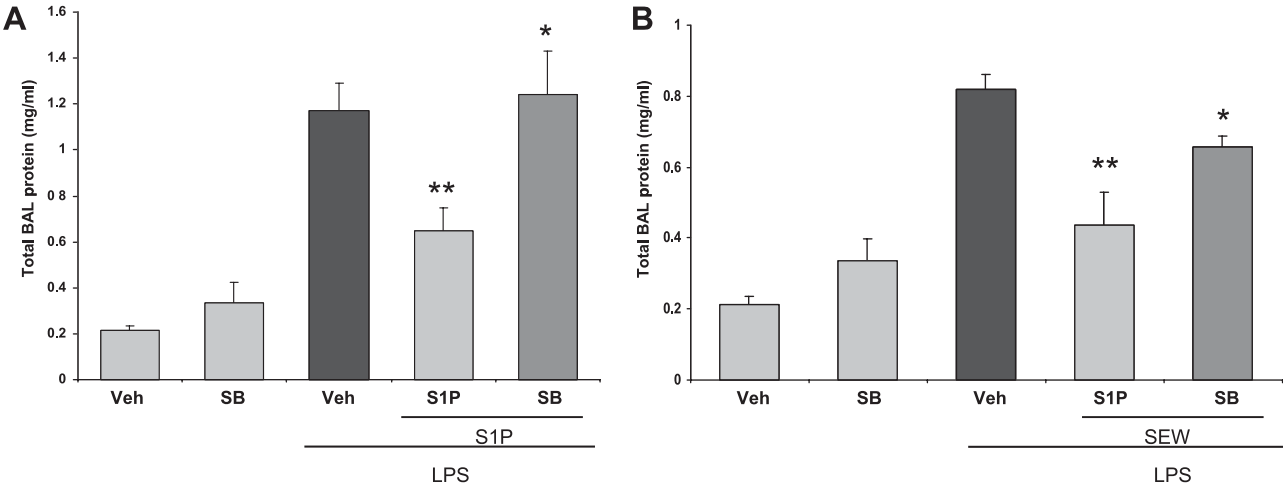

Figure 3. Effects of $S1PR_1$ inhibition on S1P/SEW-2871–mediated barrier enhancement. In these experiments, 8–10-week-old C57Bl/6 mice were treated with 0.1 mg/mouse SB-649146 (intravenous) 30 minutes after challenge with LPS, LPS/S1P, or LPS/SEW-2871. Mice were killed 18 hours later, and BAL fluid was collected for evaluation of protein levels. (*A*) The administration of 0.1 mg/mouse of SB-649146 completely reversed S1P-mediated barrier enhancement properties, as reflected by raising BAL total protein concentrations significantly (*$P = 0.034$, S1P/LPS/SB-649146 versus S1P/LPS; **$P \leq 0.05$, S1P/LPS versus LPS). (*B*) Administering 0.1 mg/mouse of SB-649146 attenuates the barrier-protective effects of SEW-2871 significantly in LPS-challenged mice, as reflected by significant increase in BAL total protein level (*$P = 0.044$, SEW-2871/LPS/SB-649146 versus SEW/LPS; **$P \leq 0.05$, SEW-2871/LPS versus LPS) ($n = 4$).

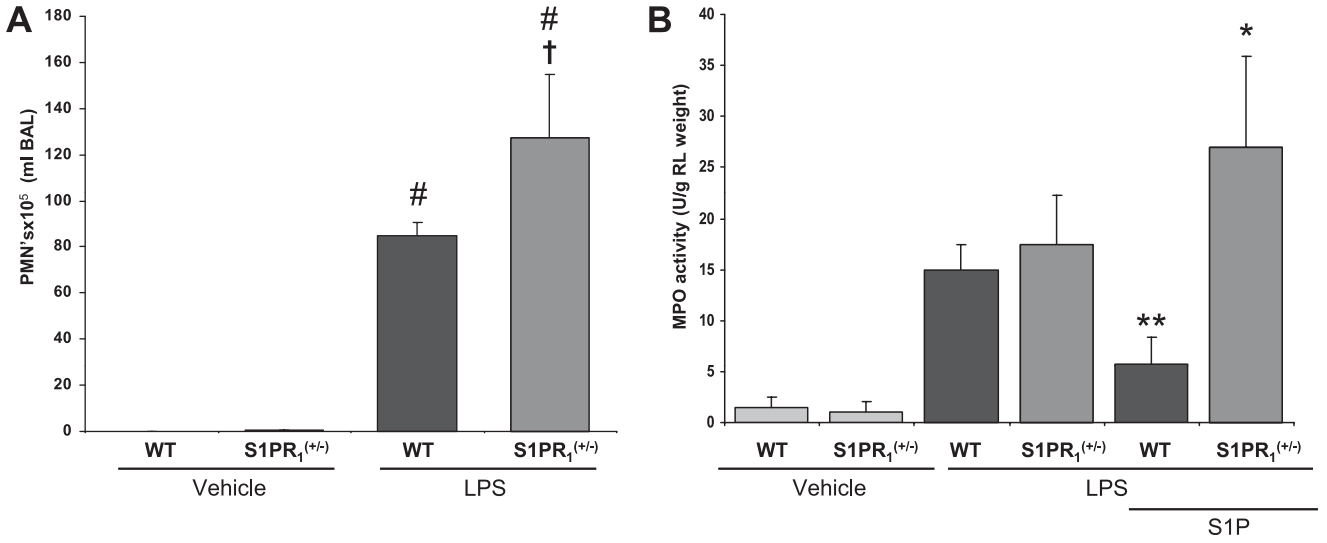

Figure 4. Responses of $S1PR_1^{+/-}$ heterozygous mice to murine LPS-induced acute lung injury. (*A*) $S1PR_1^{+/-}$ or wild-type (WT) mice were challenged with LPS (intratracheally) and killed 18 hours later. Disruption of vascular barrier integrity was reflected by significant increase in BAL PMNs of $S1PR_1^{+/-}$ mice compared with WT mice ($^{\#,\dagger}P \leq 0.05$, $S1PR_1^{+/-}$/LPS versus LPS; $^{\#}P \leq 0.05$, $S1PR_1$/LPS versus $S1PR_1^{+/-}$/vehicle). (*B*) Effects of S1P on lung tissue myeloperoxidase (MPO) activity in $S1P_1^{+/-}$ heterozygous mice challenged with LPS. $S1PR_1^{+/-}$ or wild-type mice were treated with an intravenous injection of S1P 30 minutes after LPS. As reflected by lung-tissue MPO activity, barrier-enhancing properties of S1P were significantly attenuated in LPS-challenged $S1PR_1^{+/-}$ mice compared with WT mice (*$P \leq 0.05$, WT-LPS versus WT-LPS/S1P; **$P \leq 0.05$, WT-S1P/LPS versus $S1PR_1^{+/+}$-S1P/LPS).

sion (17), ventilation-induced lung injury (VILI) (18, 19), and ionizing radiation (20, 21). Furthermore, $S1PR_1$ ligation is critical to hepatocyte growth factor–mediated, hyaluronan-mediated, and activated protein C–mediated EC barrier enhancement via $S1PR_1$ transactivation (11, 12,
31). In contrast, the ligation of $S1PR_3$ induces Rho GTPase signaling to the cytoskeleton and increased lung permeability (37, 39, 40), and $S1PR_3$ is transactivated by Mu opioid receptors and specific isoforms of CD44, resulting in increased vascular permeability (12, 41). The role of $S1PR_2$ in lung-barrier regulation is not well understood, but $S1PR_2$ was suggested to evoke signals similar to those of $S1PR_3$, which increases vascular leakage (42). To facilitate the translation of *in vitro* and *in vivo* information on the role of S1P/S1PRs into the pathobiology of ALI, we assessed the dose-dependent effects of S1P as well as delivery route–dependent responses (intratracheal versus intravenous) in targeting alveolar and vascular barriers. In addition, we used a selective $S1PR_1$ agonist (SEW-2871), a selective $S1PR_1$ inverse agonist (SB-649146), and genetically engineered S1PR mutant mice to assess the differential role of S1P receptors in vascular leakage in a murine model of inflammatory lung injury. The direct intratracheal or intravenous administration of S1P or SEW-2871 at less than 0.3 mg/kg significantly reduced LPS-induced murine lung inflammation and permeability. However, the intratracheal delivery of S1P at 0.5 mg/kg resulted in significant alveolar–capillary barrier disruption, with pulmonary edema and markedly elevated protein concentrations. Furthermore, the intratracheal administration of S1P at 2 mg/kg produced rapid lethality (2 mg/kg). These results differed somewhat from those of a report (37) concluding that the exposure of pulmonary epithelium to S1P (2 mg/kg) by intratracheal injection induces acute pulmonary edema (PE) PE, as reflected by the extravasation of Evans blue dye into the airways, and by comparisons of wet/dry weight ratios. The S1P-induced PE in this report was more severe than the LPS-induced PE, but was not lethal. Despite greater $S1PR_1$ selectivity, our results indicate that

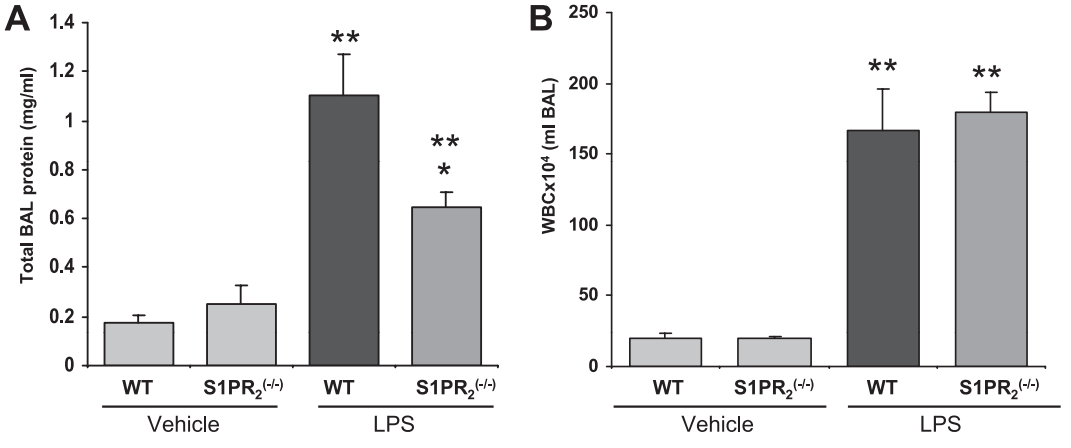

Figure 5. Responses of $S1PR_2^{-/-}$ knockout (KO) mice to murine LPS-induced acute lung injury. BAL was collected 18 hours after intratracheal injection of LPS, and total protein level was measured in $S1PR_2^{-/-}$ KO and WT $S1P^{+/+}$ mice. (*A*) BAL protein concentration in $S1PR_2^{-/-}$ KO mice was significantly lower (*$P = 0.02$ and **$P \leq 0.05$ LPS versus vehicle) than in WT mice, supporting our hypothesis of the barrier-disruptive role of $S1P_2$ receptors. (*B*) No changes occurred in white blood cell counts in $S1PR_2^{-/-}$ KO mice compared with WT mice.

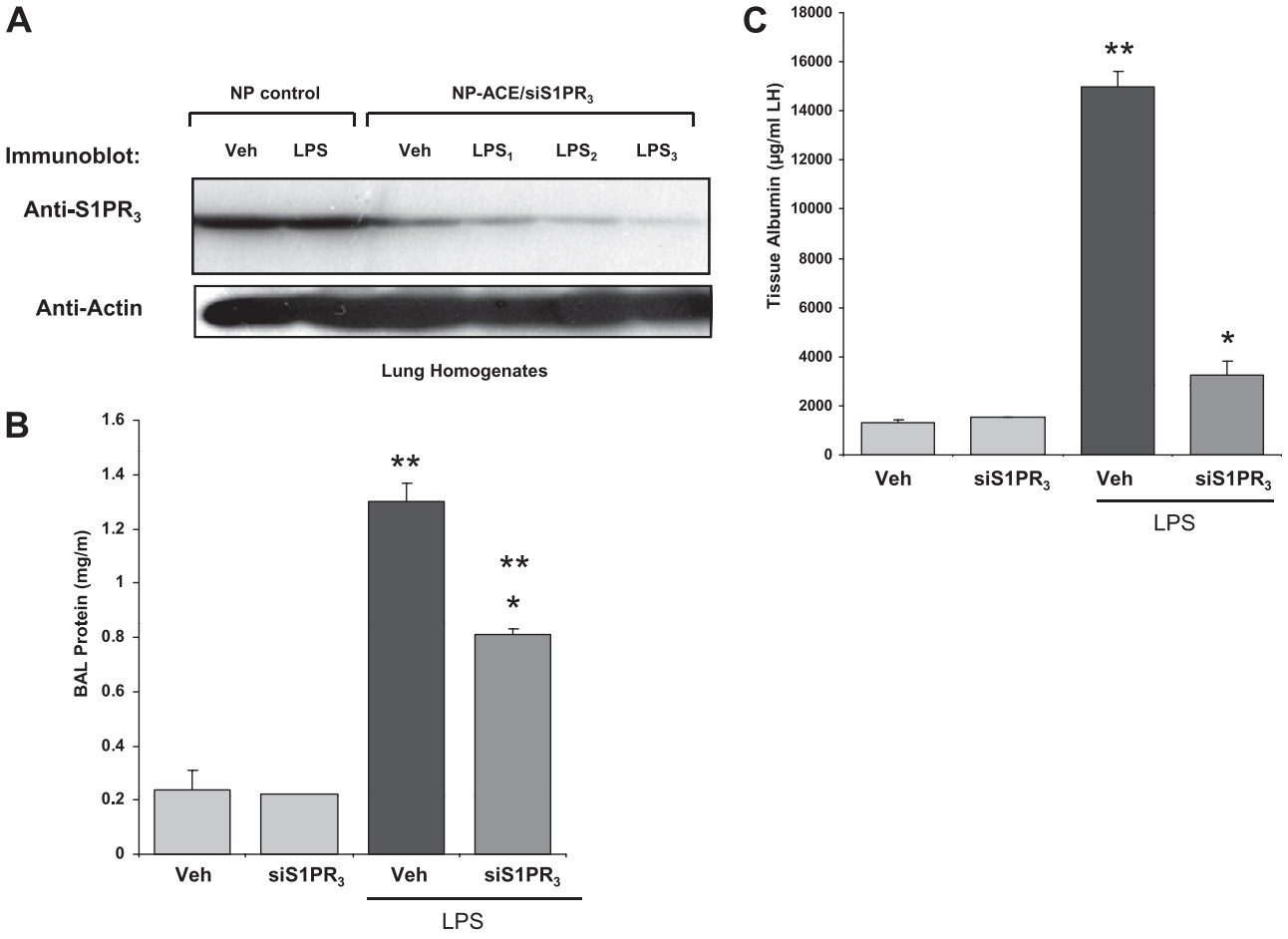

Figure 6. LPS-induced acute lung injury responses in mice with $S1PR_3$ silencing via angiotensin-converting enzyme (ACE) antibody–conjugated nanocarriers with short, interfering RNA (siRNA)–$S1P_3$ cargo. (*A*) Western blot analysis of lung tissue after ACE antibody–conjugated nanocarrier delivery of siRNA targeting $S1PR_3$. Nanocarriers were injected into jugular veins to deliver 10 mg/kg $S1PR_3$ siRNA specifically into lung vessels, and after 5 days, tissues were assessed by examining lung homogenates by immunoblotting in control (NP control) and in siS1PR3-depleted murine lungs. (*B*) Lung injury induced by LPS is attenuated by intravenous injection of $S1PR_3$ siRNA, using ACE antibody–conjugated nanoparticle delivery as reflected by BAL albumin content (*$P < 0.01$) compared with LPS controls. **$P < 0.05$ in $siS1PR_3$/vehicle versus LPS injured mice. (*C*) Graphic representation of tissue albumin content indicates ACE antibody–conjugated nanocarrier delivery significantly reduces tissue albumin content in LPS-induced lung injury (*$P < 0.01$) compared with the LPS group. **$P < 0.05$, significant increases in tissue albumin after LPS, compared with $siS1PR_3$ control mice.

intratracheally delivered SEW-2871 at 0.5 mg/kg also resulted in significant alveolar–capillary barrier disruption, but was not lethal at 2 mg/kg. Consistent with the $S1PR_1$ regulation of alveolar/vascular barrier function, wild-type mice pretreated with the $S1PR_1$ inverse agonist, SB-649146, or $S1PR_1{}^{+/-}$ mice exhibited a loss of S1P/SEW-2871–mediated barrier protection after a challenge with LPS, whereas the instillation of SB-649146 alone had no effect on BAL fluid protein concentrations. The inability of SB-649146 to increase total BAL protein on its own suggests that this inverse agonist, at low concentrations, may bind to $S1PR_1$ without affecting basal $S1PR_1$ signaling, compared with high concentrations of the inverse agonist, which are expected to stimulate an inverse agonism of $S1PR_1$ signaling. The submaximal level of inverse agonism used under the present experimental conditions allowed for the observed antagonist effect on S1P-mediated signaling thorough $S1PR_1$, as demonstrated by the ability of SB-649146 to attenuate the $S1PR_1$ response of SEW-2871.

In contrast to $S1PR_1$, the ligation or transactivation of $S1PR_2$ and $S1PR_3$ was observed to evoke barrier-disruptive responses. We demonstrated that the activation of $S1PR_3$, which is expressed in both alveolar epithelium and lung vascular endothelium (37), leads to robust Rho/Rho kinase–mediated EC barrier disruption (12, 37). Furthermore, the $S1PR_3$ receptor is implicated in the untoward effects of FTY-720, an S1P analogue, when administered to some humans with multiple sclerosis who experience bradycardia, airway hyperreactivity, and sporadic glomerulonephritis. Consistent with the ascribed roles of these S1P receptors, our study determined that $S1PR_2{}^{-/-}$ KO mice as well as mice with reduced $S1PR_3$ expression (via ACE antibody–conjugated, $siS1PR_3$-containing nanocarriers), confirms that the physiologic role of S1PR3 receptors is barrier-disruptive. Our study also suggests that barrier disruption may ensue in pharmacologic situations when the higher-affinity $S1PR_1$ receptor is saturated by high doses of S1P or S1P analogues such as FTY-720 and the phosphorylated form of FTY-720 (FTY-720-P), which acts as an agonist for S1PRs (43, 44). In particular, the (S)-enantiomer of FTY-720-P binds to $S1PR_1$, $S1PR_3$, $S1PR_4$, and $S1PR_5$, but not $S1PR_2$, with high affinity, compared with the (R)-enantiomer of FTY-720-P (45). Although FTY-720-P lacks binding to $S1PR_2$, it is unclear whether it mimics all the biological effects of S1P, such as maintenance of vascular tone, endothelial barrier integrity, and anti-inflammatory responses, with a similar or higher potency

in vivo in vascular systems. Interestingly, the down-regulation of $S1PR_1$ by (S)-FTY-720-P seems to be maintained longer than by S1P in Chinese hamster ovary cells stably expressing $S1PR_1$ (46). Further studies comparing the actions of S1P, FTY-720-P, and other S1P analogues should provide new therapeutic approaches for ameliorating vascular inflammatory diseases.

In conclusion, our study confirms the therapeutic potential of S1P and S1P analogues with $S1P_1$ specificity in inflammatory lung injury. In addition, the results underscore the critical nature of the route of S1P administration and S1P dose, as well as a requirement for $S1PR_1$ selectivity. At physiologically relevant concentrations, S1P is barrier-protective, regardless of delivery via intratracheal or intravenous routes. The activation of $S1P_2$ and $S1P_3$ receptors, however, contributes to alveolar and vascular barrier disruption, whereas the targeted deletion or silencing of $S1P_2$ and $S1P_3$ receptors was found to be beneficial. These results suggest that the consideration of a combined therapeutic approach involving an $S1P_1$ agonist and an $S1P_2$ or $S1P_3$ receptor antagonist (or siRNA) may be of potential utility. Continued clarification of the exact roles of S1PRs in ALI pathobiology will greatly facilitate the development of S1P-based therapies for the critically ill, as well as pharmacogenomic approaches to alleviating disturbed lung fluid balance.

Author Disclosure: None of the authors has a financial relationship with a commercial entity that has an interest in the subject of this manuscript.

Acknowledgments: The authors thank Dr. Richard L. Proia (National Institutes of Health, Bethesda, MD) for providing $S1PR_1^{+/-}$ heterozygous and $S1PR_2^{-/-}$ KO mice. The authors also thank Bolot Mambetsariev, PhD, for skilled technical assistance.

References

1. Brower RG. Mechanical ventilation in acute lung injury and ARDS: tidal volume reduction. *Crit Care Clin* 2002;18:1–13.
2. Goss CH, Brower RG, Hudson LD, Rubenfeld GD. Incidence of acute lung injury in the United States. *Crit Care Med* 2003;31:1607–1611.
3. Matthay MA, Zimmerman GA, Esmon C, Bhattacharya J, Coller B, Doerschuk CM, Floros J, Gimbrone MA Jr, Hoffman E, Hubmayr RD, *et al.* Future research directions in acute lung injury: summary of a National Heart, Lung, and Blood Institute working group. *Am J Respir Crit Care Med* 2003;167:1027–1035.
4. Dreyfuss D, Saumon G. Ventilator-induced lung injury: lessons from experimental studies. *Am J Respir Crit Care Med* 1998;157:294–323.
5. Carlton DP, Cummings JJ, Scheerer RG, Poulain FR, Bland RD. Lung overexpansion increases pulmonary microvascular protein permeability in young lambs. *J Appl Physiol* 1990;69:577–583.
6. Dreyfuss D, Soler P, Basset G, Saumon G. High inflation pressure pulmonary edema. Respective effects of high airway pressure, high tidal volume, and positive end-expiratory pressure. *Am Rev Respir Dis* 1988;137:1159–1164.
7. Parker JC, Hernandez LA, Longenecker GL, Peevy K, Johnson W. Lung edema caused by high peak inspiratory pressures in dogs: role of increased microvascular filtration pressure and permeability. *Am Rev Respir Dis* 1990;142:321–328.
8. Parker JC, Hernandez LA, Peevy KJ. Mechanisms of ventilator-induced lung injury. *Crit Care Med* 1993;21:131–143.
9. Garcia JG, Liu F, Verin AD, Birukova A, Dechert MA, Gerthoffer WT, Bamburg JR, English D. Sphingosine 1–phosphate promotes endothelial cell barrier integrity by EDG-dependent cytoskeletal rearrangement. *J Clin Invest* 2001;108:689–701.
10. Dudek SM, Jacobson JR, Chiang ET, Birukov KG, Wang P, Zhan X, Garcia JG. Pulmonary endothelial cell barrier enhancement by sphingosine 1–phosphate: roles for cortactin and myosin light chain kinase. *J Biol Chem* 2004;279:24692–24700.
11. Singleton PA, Dudek SM, Chiang ET, Garcia JG. Regulation of sphingosine 1–phosphate–induced endothelial cytoskeletal rearrangement and barrier enhancement by S1P1 receptor, Pi3 kinase, Tiam1/Rac1, and alpha-actinin. *FASEB J* 2005;19:1646–1656.
12. Singleton PA, Dudek SM, Ma SF, Garcia JG. Transactivation of sphingosine 1–phosphate receptors is essential for vascular barrier regulation: novel role for hyaluronan and CD44 receptor family. *J Biol Chem* 2006;281:34381–34393.
13. Schaphorst KL, Chiang E, Jacobs KN, Zaiman A, Natarajan V, Wigley F, Garcia JG. Role of sphingosine-1 phosphate in the enhancement of endothelial barrier integrity by platelet-released products. *Am J Physiol Lung Cell Mol Physiol* 2003;285:L258–L267.
14. McVerry BJ, Peng X, Hassoun PM, Sammani S, Simon BA, Garcia JG. Sphingosine 1–phosphate reduces vascular leak in murine and canine models of acute lung injury. *Am J Respir Crit Care Med* 2004;170:987–993.
15. Peng X, Hassoun PM, Sammani S, McVerry BJ, Burne MJ, Rabb H, Pearse D, Tuder RM, Garcia JG. Protective effects of sphingosine 1–phosphate in murine endotoxin-induced inflammatory lung injury. *Am J Respir Crit Care Med* 2004;169:1245–1251.
16. Kappos L, Antel J, Comi G, Montalban X, O'Connor P, Polman CH, Haas T, Korn AA, Karlsson G, Radue EW. Oral fingolimod (FTY720) for relapsing multiple sclerosis. *N Engl J Med* 2006;355:1124–1140.
17. Sanchez T, Estrada-Hernandez T, Paik JH, Wu MT, Venkataraman K, Brinkmann V, Claffey K, Hla T. Phosphorylation and action of the immunomodulator FTY720 inhibits vascular endothelial cell growth factor–induced vascular permeability. *J Biol Chem* 2003;278:47281–47290.
18. Moreno-Vinasco L, Jacobson JR, Bonde P, Sammani S, Mirzapoiazova T, Vigneswaran WT, Garcia JG. Attenuation of rodent lung ischemia-reperfusion injury by sphingosine 1–phosphate. *J Organ Dysfunction* 2008;4:106–114.
19. Hla T. Physiological and pathological actions of sphingosine 1–phosphate. *Semin Cell Dev Biol* 2004;15:513–520.
20. Liu F, Verin AD, Wang P, Day R, Wersto RP, Chrest FJ, English DK, Garcia JG. Differential regulation of sphingosine-1–phosphate– and VEGF-induced endothelial cell chemotaxis: involvement of G (ialpha2)-linked Rho kinase activity. *Am J Respir Cell Mol Biol* 2001;24:711–719.
21. Rosen H, Goetzl EJ. Sphingosine 1–phosphate and its receptors: an autocrine and paracrine network. *Nat Rev Immunol* 2005;5:560–570.
22. Nonas SA, Moreno-Vinasco L, Ma SF, Jacobson JR, Desai AA, Dudek SM, Flores C, Hassoun PM, Sam L, Ye SQ, *et al.* Use of consomic rats for genomic insights into ventilator-associated lung injury. *Am J Physiol Lung Cell Mol Physiol* 2007;293:L292–L302.
23. Wang T, Moreno-Vinasco L, Huang Y, Lang GD, Linares JD, Goonewardena SN, Grabavoy A, Samet JM, Geyh AS, Breysse PN, *et al.* Murine lung responses to ambient particulate matter: genomic analysis and influence on airway hyperresponsiveness. *Environ Health Perspect* 2008;116:1500–1508.
24. Mirzapoiazova T, Kolosova IA, Moreno L, Sammani S, Garcia JG, Verin AD. Suppression of endotoxin-induced inflammation by taxol. *Eur Respir J* 2007;30:429–435.
25. Moitra J, Evenoski C, Sammani S, Wadgaonkar R, Turner JR, Ma SF, Garcia JG. A transgenic mouse with vascular endothelial overexpression of the non-muscle myosin light chain kinase-2 isoform is susceptible to inflammatory lung injury: role of sexual dimorphism and age. *Transl Res* 2008;151:141–153.
26. Meyer NJ, Huang Y, Singleton PA, Sammani S, Moitra J, Evenoski CL, Husain AN, Mitra S, Moreno-Vinasco L, Jacobson JR, *et al.* Gadd45a is a novel candidate gene in inflammatory lung injury via influences on Akt signaling. *FASEB J* 2009;23:1325–1333.
27. Waters CM, Long J, Gorshkova I, Fujiwara Y, Connell M, Belmonte KE, Tigyi G, Natarajan V, Pyne S, Pyne NJ. Cell migration activated by platelet-derived growth factor receptor is blocked by an inverse agonist of the sphingosine 1–phosphate receptor-1. *FASEB J* 2006;20:509–511.
28. Natarajan V, Jayaram HN, Scribner WM, Garcia JG. Activation of endothelial cell phospholipase D by sphingosine and sphingosine-1–phosphate. *Am J Respir Cell Mol Biol* 1994;11:221–229.
29. English D, Welch Z, Kovala AT, Harvey K, Volpert OV, Brindley DN, Garcia JG. Sphingosine 1–phosphate released from platelets during clotting accounts for the potent endothelial cell chemotactic activity of blood serum and provides a novel link between hemostasis and angiogenesis. *FASEB J* 2000;14:2255–2265.
30. Jang C, Koh YJ, Lim NK, Kang HJ, Kim DH, Park SK, Lee GM, Jeon CJ, Koh GY. Angiopoietin-2 exocytosis is stimulated by sphingosine-1–phosphate in human blood and lymphatic endothelial cells. *Arterioscler Thromb Vasc Biol* 2009;29:401–407.
31. Finigan JH, Dudek SM, Singleton PA, Chiang ET, Jacobson JR, Camp SM, Ye SQ, Garcia JG. Activated protein c mediates novel lung endothelial barrier enhancement: role of sphingosine 1–phosphate receptor transactivation. *J Biol Chem* 2005;280:17286–17293.

32. Brinkmann V. Sphingosine 1–phosphate receptors in health and disease: mechanistic insights from gene deletion studies and reverse pharmacology. *Pharmacol Ther* 2007;115:84–105.
33. McVerry BJ, Garcia JG. *In vitro* and *in vivo* modulation of vascular barrier integrity by sphingosine 1–phosphate: mechanistic insights. *Cell Signal* 2005;17:131–139.
34. Pyne S, Pyne NJ. Sphingosine 1–phosphate signalling in mammalian cells. *Biochem J* 2000;349:385–402.
35. Spiegel S, Milstien S. Sphingosine-1–phosphate: an enigmatic signalling lipid. *Nat Rev Mol Cell Biol* 2003;4:397–407.
36. Berdyshev EV, Gorshkova IA, Garcia JG, Natarajan V, Hubbard WC. Quantitative analysis of sphingoid base-1–phosphates as bisacetylated derivatives by liquid chromatography–tandem mass spectrometry. *Anal Biochem* 2005;339:129–136.
37. Singleton PA, Moreno-Vinasco L, Sammani S, Wanderling SL, Moss J, Garcia JG. Attenuation of vascular permeability by methylnaltrexone: role of MOp-r and S1P3 transactivation. *Am J Respir Cell Mol Biol* 2007;37:222–231.
38. Gon Y, Wood MR, Kiosses WB, Jo E, Sanna MG, Chun J, Rosen H. S1P3 receptor–induced reorganization of epithelial tight junctions compromises lung barrier integrity and is potentiated by TNF. *Proc Natl Acad Sci USA* 2005;102:9270–9275.
39. Shikata Y, Birukov KG, Birukova AA, Verin A, Garcia JG. Involvement of site-specific Fak phosphorylation in sphingosine-1 phosphate– and thrombin-induced focal adhesion remodeling: role of Src and Git. *FASEB J* 2003;17:2240–2249.
40. Shikata Y, Birukov KG, Garcia JG. S1p induces FA remodeling in human pulmonary endothelial cells: role of Rac, Git1, Fak and Paxillin. *J Appl Physiol* 2003;94:1193–1203.
41. Singleton PA, Lingen MW, Fekete MJ, Garcia JG, Moss J. Methylnaltrexone inhibits opiate and VEGF-induced angiogenesis: role of receptor transactivation. *Microvasc Res* 2006;72:3–11.
42. Niessen F, Furlan-Freguia C, Fernandez JA, Mosnier LO, Castellino FJ, Weiler H, Rosen H, Griffin JH, Ruf W. Endogenous EPCR/APC-par1 signaling prevents inflammation-induced vascular leakage and lethality. *Blood* 2009;113:2859–2866.
43. Brinkmann V, Lynch KR. Fty720: targeting G-protein–coupled receptors for sphingosine 1–phosphate in transplantation and autoimmunity. *Curr Opin Immunol* 2002;14:569–575.
44. Mandala S, Hajdu R, Bergstrom J, Quackenbush E, Xie J, Milligan J, Thornton R, Shei GJ, Card D, Keohane C, *et al.* Alteration of lymphocyte trafficking by sphingosine-1–phosphate receptor agonists. *Science* 2002;296:346–349.
45. Kiuchi M, Adachi K, Tomatsu A, Chino M, Takeda S, Tanaka Y, Maeda Y, Sato N, Mitsutomi N, Sugahara K, *et al.* Asymmetric synthesis and biological evaluation of the enantiomeric isomers of the immunosuppressive FTY720-phosphate. *Bioorg Med Chem* 2005;13:425–432.
46. Chiba K, Hoshino Y, Ohtsuki M, Kataoka H, Maeda Y, Matsuyuki H, Sugahara K, Kiuchi M, Hirose R, Adachi K. Immunosuppressive activity of FTY720, sphingosine 1–phosphate receptor agonist: I. Prevention of allograft rejection in rats and dogs by FTY720 and FTY720-phosphate. *Transplant Proc* 2005;37:102–106.